

Modeling of Wound Coaxial Blumlein Pulsers

José O. Rossi, *Member, IEEE*, Joaquim J. Barroso, and Mário Ueda

Abstract—Blumlein pulsed generators are well-suited devices for high-voltage pulse generation in nanosecond and microsecond ranges. These generators have been used with great success in several areas such as in breakdown tests, X-ray generation, lasers, and high-energy plasma implantation. They consist of lengths of transmission lines charged in parallel and synchronously discharged in series into the load by using single or multiple switches at the opposite line endings. The main problem with the device performance is the presence of the shield cable impedance contributing to the Blumlein power loss especially when using only one switch. The very well known technique used for minimizing these losses consists of winding the transmission lines to increase the line shielding inductance if coaxial cables are used. Therefore, herein, circuit models are presented to assess theoretically the temporal response of the wound coaxial Blumlein pulsed generators by using a SPICE circuit simulator. For model assessment, the authors used the experimental results produced by a wound coaxial Blumlein pulsed generator of 100 kV/200 A with 1.0 μ s of pulse duration constructed for applications in surface treatment of polymers and aluminum with high-energy ions.

Index Terms—Blumlein, coaxial cable, modeling, pulsed generator, SPICE simulator, transmission line.

I. INTRODUCTION

HIGH-VOLTAGE generators made of lengths of transmission lines have been built in the 1970–2000 era at many laboratories around the world using very diverse schemes with coaxial lines or parallel plates (striplines) driven by single or multiple switches. They have been used in a great variety of applications such as in X-ray generation [1], [2], lasers [3], breakdown tests [4], and voltage amplification [5]–[9]. Recently, we have demonstrated that stacked coaxial Blumlein pulsed generators with a single switch can be used in surface treatment of polymers and aluminum alloys by plasma implantation with high-energy ions as described in [10]. Therefore, the stacked Blumlein generators described in this paper consist of coaxial lines that are charged in parallel and discharged synchronously in series into the load as shown by a five-stage device in Fig. 1. The operation principle of this pulsed generator can be summarized as follows: In the initial state, the lines are positively charged, but the net output voltage across A and B is zero because of the initial voltage vector opposition as indicated in Fig. 1. As soon as the switch is closed, pulse voltages propagate down the active lines to the right. After one propagation delay time, they arrive at the output where reflections occur converting the initial vector

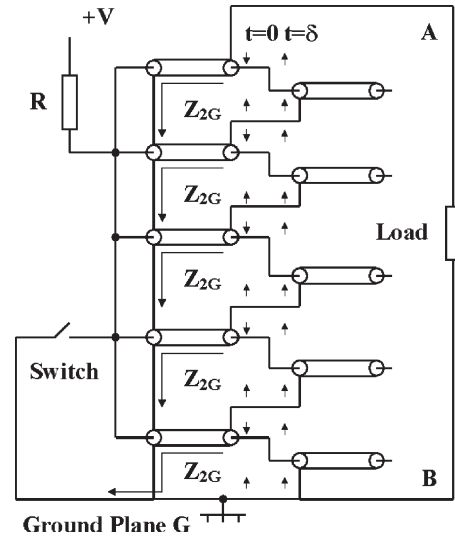


Fig. 1. Five-stage stacked coaxial Blumlein pulsed generator in single switch configuration. Z_{2G} is the impedance between the cable shield and ground.

opposition to a series addition, which persists for twice the line propagation time (2δ). This leads to an output voltage of $2nV$ for an open end or else nV for the case of a load $2nZ_0$ matched to the generator output, where n is the number of stacked Blumlein lines and $2Z_0$ is the characteristic impedance of a Blumlein line composed of two coaxial lines with impedance Z_0 connected in series at each stage. Ideally, the pulse shape would be flat during the time interval 2δ , but the appearance of parasitic impedances in this circuit configuration degrades the output pulse. This can be better explained by considering two important cable impedances in the pulsed generator configuration circuit: 1) the inner cable characteristic impedance Z_0 and 2) the impedance Z_{2G} that lies between the outer conductors of the cables and the ground plane G as shown in Fig. 1. To understand the effect of the shield parasitic impedance Z_{2G} on the pulsed generator operation, first, note that the potential difference between the shields of the top and bottom cables (see points A and B in Fig. 1) gives the output. Second, as soon as the voltage at each stage output is raised, the voltage potentials on passive line shields are increased. Third, as active lines are grounded at the switch side, the shield-distributed inductance avoids short circuits between the input and output of the cable shields when using straight lines. If $Z_{2G} \ll Z_0$, a large fraction of the output current can reach ground via cable shielding without going through the load, reducing the power delivered to the load. However, if the outer impedance Z_{2G} can be made large, for example by winding the cable on a former so that the inductance of the outer part of the jacket is high, then a higher Z_{2G} reduces the current drained from the load and, consequently, minimizes the pulse voltage droop. In this case, Z_{2G} can be described

Manuscript received November 1, 2005; revised February 25, 2006. This work was supported in part by the State of São Paulo Research Foundation (FAPESP), SP, Brazil, under Grant 00/11114-7 and in part by the Brazilian funding agencies CNPq and MCT.

The authors are with the Associated Plasma Laboratory, National Institute for Space Research, São José dos Campos, SP 12227-010, Brazil (e-mail: rossi@plasma.inpe.br).

Digital Object Identifier 10.1109/TPS.2006.881306

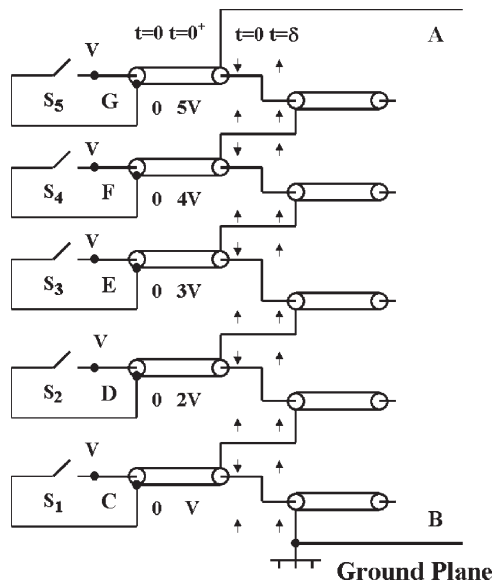


Fig. 2. Multiswitch configuration for a five-stage stacked coaxial Blumlein pulser.

as a lumped impedance given by sL , s being the Laplace operator and L being the shield self-inductance of each wound coaxial cable. In this analysis, the cables are considered to be sufficiently apart from each other to avoid isolation problems (as the voltage potential varies along the cable shields) and to make negligible the effect of mutual inductance between them. Anyway, the presence of Z_{2G} represents a serious drawback of the single switch configuration since it is impossible to eliminate the pulse droop completely because L cannot reach an infinite value. On the other hand, the use of a single switch is the major advantage of this system, which reduces cost and avoids the use of more complex synchronized triggering drivers when using several switches.

Actually, pulse droop is never completely suppressed even with multiple switching, although the overall loss of the device is less pronounced for this type of configuration. The reason for that is due to distributed capacitance formed between the outer conductors of the cables and ground. This is illustrated in Fig. 2, which shows a similar five-stage coaxial Blumlein with each active line triggered by a switch. In the initial state, the inner conductors of the cables are charged at a potential V with the corresponding shieldings at the ground potential. Immediately after the switch is closed, the terminations of the cable shields at the switch side (points C, D, E, F, and G) are charged respectively to V , $2V$, $3V$, $4V$, and $5V$, and the potential difference given by nV propagates down each corresponding n th cable shielding, charging the parasitic capacitances formed between the respective cable outer conductors and ground. Since the energy can only be provided by the passive lines, a pulse droop is produced, causing degradation and reduction of the output voltage. When the potential difference between A and B at the open ends rises to $2nV$, more energy is drained, reducing further the voltage. A quantitative study of this process is rather complex, but a qualitative analysis shows that this effect is not severe if the distributed inner line capacitance is large compared with the cable shielding capacitance. However, while

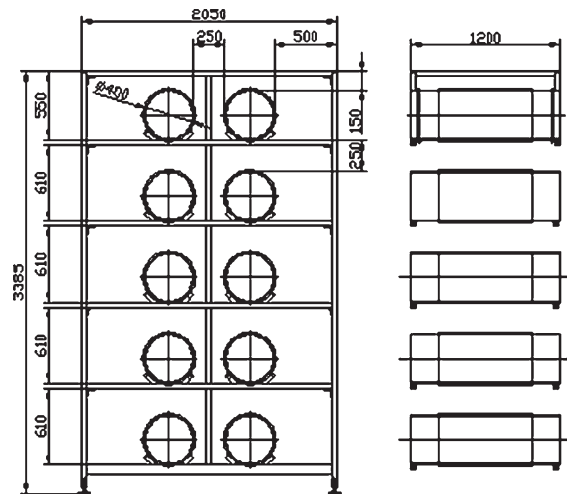


Fig. 3. Sectional view of the coaxial Blumlein pulser with dimensions in millimeters.

the equivalent inner capacitance of the active lines decreases as $1/n$, the total shielding stray capacitance decreases more slowly because C varies as the logarithm distance between the cable shields and ground. Moreover, because of the logarithm variation, additional stray braiding capacitances between the lines should be considered, even keeping lines separated by a large distance. Therefore, as reported by Fitch and Howell [11], the capacitive loading has a severe harmful effect on the device output voltage if we stack more than eight cables (i.e., for $2n > 9$) in a multiple switching configuration.

The paper is organized as follows: In Section II, a coaxial Blumlein pulser of 100 kV/200 A with pulse duration of $1.0 \mu s$ (developed for applications in plasma immersion ion implantation) is described. Two PSPICE circuit models presented in Section III are used to assess the device performance. The results are also given in this section. Then, Section IV shows a Blumlein pulser with a similar coaxial configuration but with a lower droop rate than that presented by the scheme in Fig. 1. Finally, Section V presents the conclusions of this paper.

II. BLUMLEIN PULSER

The Blumlein pulser was constructed by using ten lengths of 100-m URM67/50- Ω coaxial cables according to the schematic circuit in Fig. 1. The cables have a maximum breakdown voltage of 40 kV and were wound around cylindrical tubes made from polyvinyl chloride (PVC) and supported by an aluminum structure as shown in Fig. 3. To charge the cables, we used a compact switched-mode power supply of 35 kV with negative polarity and maximum charge rate of 8.0 kJ/s. For the switching system, a thyatron tube with 35-kV/5-kA voltage/current ratings was used. This switch incorporates a glass envelope single gap tube that conducts in the reverse direction (hollow anode version), which is an important characteristic for the pulser design as the impedance mismatch into the system caused by the shield cable impedance produces negative voltages reflected at the generator input. Due to the operation with negative polarity, we used two 60-kV isolation pulse transformers for driver/heating systems of the thyatron tube. The tube cathode is

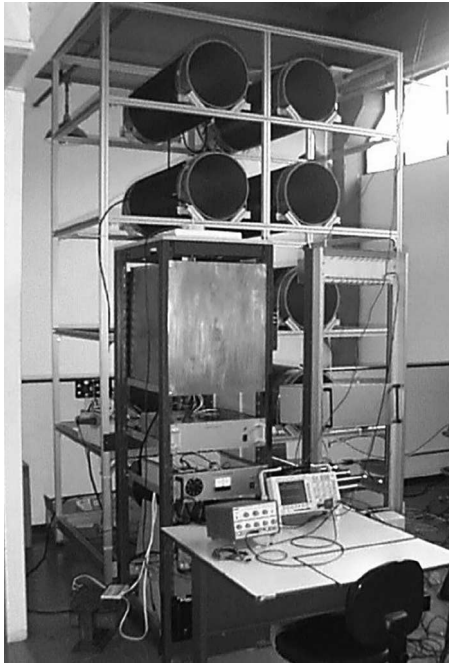


Fig. 4. Whole Blumlein system with the coaxial winding structure in the back.

also isolated from ground by a PVC support base. To make the input connections, coaxial cable shieldings are stripped back by 300 mm, and the inner conductors are connected to a small cooper plate. Then, the shieldings are joined through special connectors to a second grounded cooper plate separated from the first one by a stripped shielding distance of 300 mm. The same technique was applied to make the interstage connections where both the shieldings (or inner conductors) of adjacent cables are joined together. To reduce the thyatron connection inductance to nanohenry range, we used the outer conductors of two URM67 coaxial cables 0.7 m long connected in parallel to link the thyatron anode to the grounded plate. Similarly, both inner conductors of these cables were used to link the cathode to the first plate.

For the high-voltage tests of the pulse generator, we used as a load a noninductive resistance of 500 Ω , which consists of a continuous spiral (narrow metallic tape) wound around a flat insulator ribbon. Finally, Fig. 4 shows the whole Blumlein system described.

III. BLUMLEIN MODELS

Analytical models (based on a ladder circuit network composed of a series string of cable impedances Z_0 short circuited by cable shield impedances Z_{2G}) have been described elsewhere [12]. Despite the good performance in predicting correctly the voltage gain of the pulser, the model cannot give the temporal response of the output voltage. On the other hand, a PSPICE model given in [13], which uses ideal coaxial transmission lines to represent a parallel-plate Blumlein line configuration, was used with great success to determine the temporal response of the device. Therefore, the idea here is to use this model developed on the PSPICE simulator [14] to represent a Blumlein pulser built in a coaxial configuration

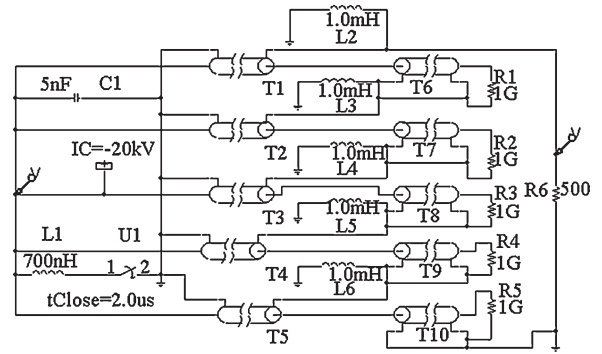


Fig. 5. PSPICE circuit model assuming Z_{2G} as a lumped inductance.

with several stages. However, in the case of Blumleins with wound cables, the cable shield impedance becomes a lumped inductance, and a good approximation is to assume Z_{2G} in a first method as a coaxial winding inductance L rather than an ideal transmission line. Later, in a second description, Z_{2G} will be represented as a transmission line.

To test the lumped-impedance model, the Blumlein pulse generator of Fig. 1 was represented as shown in Fig. 5. In this case, the active (T_1 to T_5) and passive (T_6 to T_{10}) lines are represented by ideal transmission lines of cable characteristic impedance Z_0 equal to the cable impedance of 50 Ω with a total transit time δ given by 500 ns = 100 m \times 5 ns/m (i.e., cable length times the cable delay per meter). The generator output is connected to a resistive matched load of 500 Ω for the test simulation. The open ends of the passive lines are simulated through high-value resistors (1 G Ω) to avoid node list problems in the PSPICE simulation. In relation to Z_{2G} , the cable shield impedances are represented by the inductance of each coaxial inductance measured of about $L = 1.0$ mH (see L_2 to L_6 in Fig. 5). Other important effects included in our model are those produced by the stray inductance and capacitance at the connections between switch and coaxial lines. These stray impedances cause overshoot in the beginning and end of the pulse, and when minimized, the pulse rise/fall times are only determined by the switch characteristics such as the resistance and inductance of switch plasma column [15]. Because of the great size and construction geometry used in our pulse generator, however, it was not possible to minimize the stray inductance at the switch connections below $L_1 = 700$ nH. The estimated stray capacitance obtained was of the order of $C_1 = 5$ nF. In our case, the switch was considered as an ideal on-off element device, having open and closed resistances of 1 M Ω and 0.01 Ω , respectively. Fig. 6 shows the output voltage simulation (thick line) given by the model of Fig. 5 for a charging voltage of -20 kV. For comparison, the corresponding experimental result (measured by a high-voltage probe of 1:10 000) is also given in the same figure by the thin line. Here, we observe that there is an excellent agreement between both curves. The difference is almost imperceptible during the pulse, but after pulse duration, we see a slight disagreement. To understand this, first, we need to consider the oscillatory response after the pulse cessation. The oscillatory response arises from a mismatch of the cable shield inductance at the output of each active line. After the switch is closed, a negative pulse propagates toward the end of

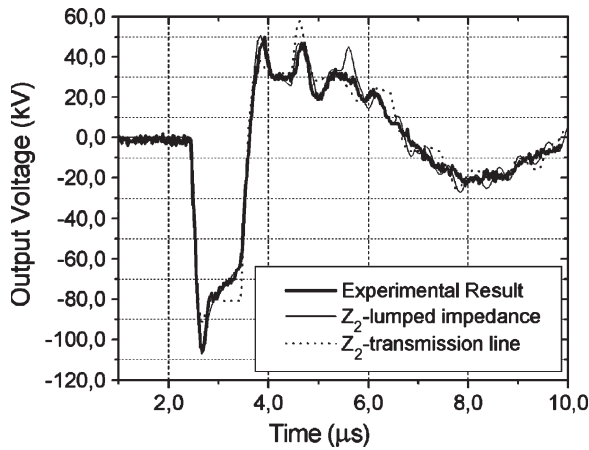


Fig. 6. Experimental and simulation results of the output voltage for charging voltage of -20 kV.

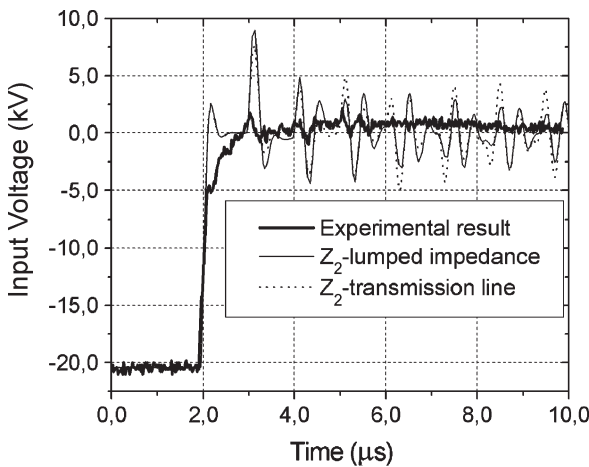


Fig. 7. Experimental and simulation results of the input voltage for the corresponding output voltage of Fig. 6.

the active line. When the pulse arrives there, it sees a mismatch caused by lumped inductance of the cable shield, generating a reflected pulse of same polarity that travels back the active line toward the input. As soon as the reflected pulse reaches the input, it reverses polarity (because this side is short circuited by the switch) and propagates down the line to the output. Therefore, after a delay of two line propagation times, the reflected pulse arrives at the output producing a positive voltage and a subsequent reflection that propagates back again, undergoing the same process described. Of course, the continuation of this process provides an oscillatory response with decreasing amplitude in time, which is the sum of all pulse voltages that appear at the output terminals of all active and passive lines. The discrepancies between the simulation and experimental results in the tail of the output pulse can be accounted for the fact that PSPICE model does not include any losses (radiation and resistance) in transmission lines or in the cable connections. This effect is more evident at the input voltage of the Blumlein, where Fig. 7 shows the input voltage simulation (thin line) and the corresponding experimental waveform (thick line) taken at the Blumlein stack input. The voltage marker in PSPICE

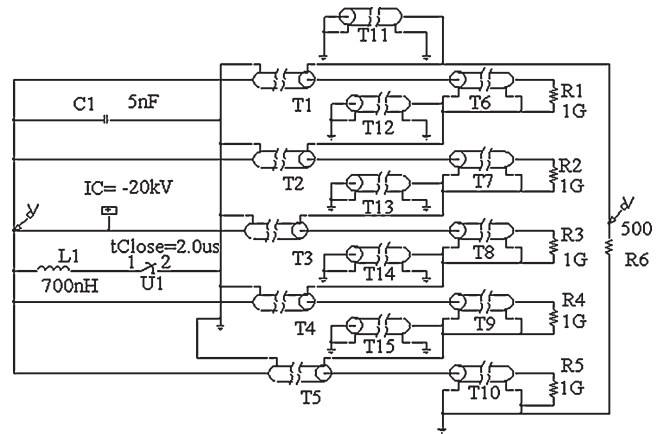


Fig. 8. PSPICE circuit model assuming Z_{2G} as a transmission line.

circuit of Fig. 5 indicates clearly the point of measurement, which includes the stray impedances (L_1 and C_1) of two short coaxial cables (700 cm) used to make the switch connections. Because of the stray impedances and reflected pulses coming from output, the input voltage oscillates. In practice, however (as shown in Fig. 7), the oscillations are strongly damped, and the pulse rise time is increased due to the ohmic losses (R) present in the transmission lines, such as in a damped inductance–capacitance (LC) oscillatory circuit.

In the second description that follows, we assume a transmission-line representation for Z_{2G} , in which cable shield impedances are represented by ideal transmission lines laid between the adjacent pulser lines (see lines T_{11} to T_{15} in Fig. 8). As each cable shielding at the switch side is grounded, the parasitic lines are also short circuited at their input by grounding the inner conductors of the lines. In the simulation, the parasitic-line characteristic impedance is equal to impedance of the cable shield given by $\sqrt{L/C}$, where L is the coil inductance and C is the equivalent coil capacitance with regard to the ground plane. In addition, it is assumed that all the parasitic lines have the same transit time $T = \sqrt{LC}$. By using the estimated values of $L \approx 1$ mH and $C \approx 242$ pF derived in the Appendix, we tested the model with $Z_{2G} \approx 2$ k Ω and $T \approx 500$ ns. The corresponding output and input voltage simulations obtained for a charging voltage of -20 kV are shown by the dashed curves in Figs. 6 and 7, respectively. The input voltage simulation is consistent with the oscillations obtained previously for Z_{2G} lumped-element analysis. However, for the output voltage, we clearly note discrepancies between the simulation and experimental results since the simulated curve does not give the correct value of the peak, presenting a step-like shape without the pulse decay. To illustrate more clearly this effect and the pulse droop, we show in Fig. 9 the output voltage obtained for a lower charge voltage of -5 kV in an expanded scale with the stray capacitance C_1 minimized at the switch connection. In this case, the overshoot is suppressed, but the pulse still has a rise time of the order of 400 ns due to the presence of the stray inductance. We can infer from Fig. 8 that the lumped-impedance model predicts the pulse droop with good accuracy. There is an amplitude decay from -22.5 to -17.5 kV approximately, e.g., a droop rate of about 22%.

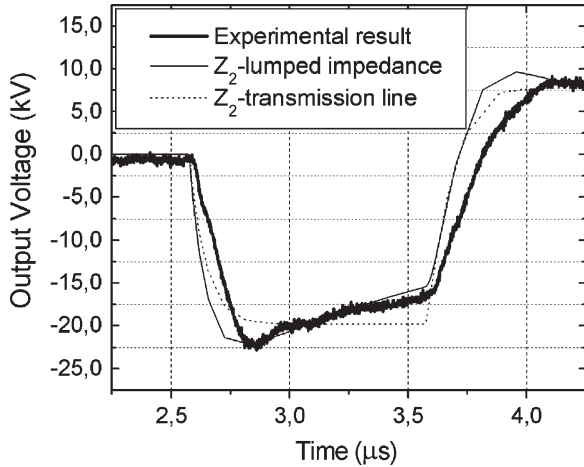


Fig. 9. Experimental and simulation output voltages for a lower charging voltage of -5 kV for the circuit in Fig. 8.

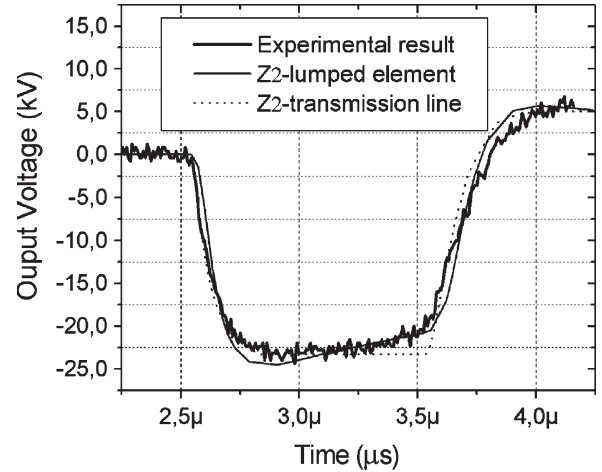


Fig. 11. Pulse output voltage for lower droop rate configuration for a charging voltage of 5 kV.

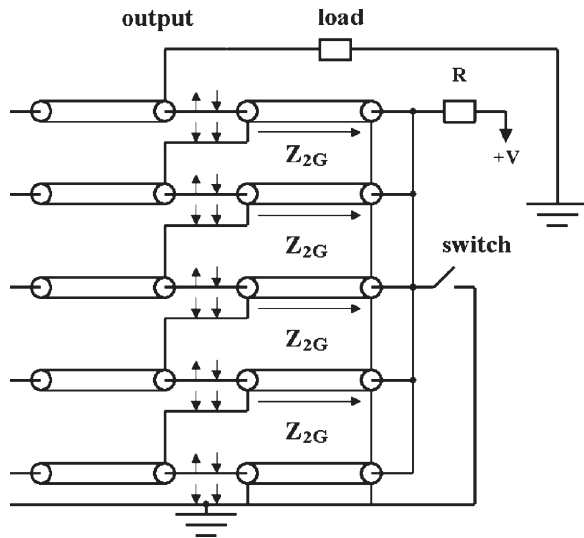


Fig. 10. Blumlein configuration with lower droop rate.

IV. CONFIGURATION WITH LOWER DROOP

Opposite polarity can be produced by grounding point A in Fig. 1 and collecting the output voltage at B instead of A. Another possible configuration for polarity inversion is depicted in Fig. 10, where the line stack is assembled grounding both sides of the bottom active line. Only four leaking paths (represented by impedance Z_{2G}) are formed in this case, resulting in a lower pulse droop rate when compared with the first configuration with five leaking paths shown in Fig. 1. The pulse droop rate of this new configuration (Fig. 10) is given in Fig. 11, where the output voltage is displayed for a charging voltage of the order of $+5$ kV with the stray capacitance minimized at the switch connection. Again, the experimental result was compared with the PSPICE models by assuming Z_{2G} as lumped impedance or ideal coaxial transmission. In this lower droop case, we note that the transmission-line model reproduces with good accuracy the initial peak of the output voltage, but as again, the lumped model provides a better fitting. Compared with Fig. 9, we see in Fig. 11 a lower droop rate since the voltage drops from 22.5 kV to only 20.0 kV, which gives a percentage fractional

droop rate of the order of 11%. To understand how the droop rate varies with the inductance of the cable windings, we can use a generalized expression that correlates the output voltage as a function of the number of stacked Blumlein n , the inner cable characteristic impedance Z_0 , the pulse duration t_p , and the coaxial winding inductance L . This expression is an adaptation of the formula used to calculate the droop rate voltage for a transmission-line transformer with a generic number of lines n described in [16], i.e.,

$$V_{OUT} = nV \exp\left(-\frac{Z_0 t_p}{2nL} \sum_1^{n-1} (n-1)^2\right). \quad (1)$$

The corresponding theoretical droop rate D is calculated from (1) such as

$$D = 1 - \exp\left(-\frac{Z_0 t_p}{2nL} \sum_1^{n-1} (n-1)^2\right). \quad (2)$$

Putting into (2) $Z_0 = 50 \Omega$, $L = 1.0$ mH, $t_p = 1.0 \mu\text{s}$, and $n = 5$ gives a droop rate of the order of the order of 14%, which is in a reasonable agreement with the corresponding experimental value of 11% measured in Fig. 11.

On the other hand, for the conventional Blumlein presented in Fig. 1, note that the droop rate calculation is easily made by replacing the term $(n-1)^2$ by n^2 in (2) since the circuit in Fig. 1 has n impedances Z_{2G} instead of $(n-1)$ as in Fig. 10. Then, the droop rate calculation now becomes

$$D = 1 - \exp\left(-\frac{Z_0 t_p}{2nL} \sum_1^n n^2\right). \quad (3)$$

By taking the same values as before for (2), we obtain from (3) a droop rate of about 24%, which is in close agreement with the measured one in Fig. 9 of approximately 22%. As the droop rate D increases with the exponent in (3), this exponential factor is higher for conventional configuration due to the rate decay dependence on the term $\sum n^2 > \sum (n-1)^2$. In practice, we obtained a droop rate reduction of 50% ($11/22$) compared with

the theoretical prediction of the order of 58% (14/24), which indicates a reasonable accuracy of the droop rate modeling proposed here.

V. CONCLUSION

In this paper, we have presented two PSPICE models to describe temporal response of wound coaxial Blumlein pulses. The first model assumes that the cable shielding impedance can be represented by a lumped impedance, whereas the second one deals with a representation in the form of a transmission-line element. We have also shown that the lumped-impedance model gives a better performance since it predicts correctly the pulse droop caused by the presence of the cable shield impedance. The transmission line presents a pulse response with a step-like shape, and in this way, it is more suitable for straight-line configuration. In practice, Blumlein pulsers are constructed by using coaxial or parallel-plate (striplines) configurations. Consequently, both models are valid for coaxial and parallel-plate configurations, and the application of one specific model (lumped impedance or transmission line) will depend on the use of either straight or wound lines. Moreover, we have demonstrated that the stray impedances (L_1 and C_1) at the switch connections limit the pulse rise time and cause an overshoot on the output pulse voltage. For example, the experimental result in Fig. 5 gives a pulse rise time of the order of 400 ns, which is compatible with the free oscillatory formula given by $T = 2\pi\sqrt{L_1 C_1}$, with the estimated stray capacitance C_1 of approximately 5 nF and the measured stray inductance L_1 of about 700 nH [10]. Minimizing the stray capacitance suppresses the overshoot, but the pulse rise time remains of the same order (400 ns) as shown by Figs. 9 and 11. Finally, we described in the previous section a different coaxial line configuration with lower droop rate than that depicted in Section III. By using this new pulser configuration, we were able to reduce the fractional droop rate from 22% to 11% at the same charging conditions of about 5 kV. In conclusion, we have shown that the models presented in this paper find important applications in the design and construction of Blumlein pulsers, using circuit configurations with wound or straight coaxial lines as well as parallel plates.

APPENDIX

CALCULATION OF THE IMPEDANCE Z_{2G}

The dimensions of the helical coil were chosen to yield a high-impedance $Z_{2G} = \sqrt{L/C}$ by making the inductance L large while keeping the capacitance C low. This was achieved by winding the cable 80 turns onto a 40-cm-diameter PVC tube 100 cm long. The winding inductance is given by the usual expression for a cylindrical coil of n turns, i.e.,

$$L = \frac{\mu_0 n^2 \pi d^2}{4l} \quad (\text{A1})$$

where $\mu_0 = 4\pi \times 10^{-7}$ H/m is the free-space magnetic permeability for the air core winding, n is the number of turns, d is the coil outer diameter, and l is the coil length. For our case, using this expression with $d \approx 40$ cm, $n = 80$, and $l \approx 100$ cm gives

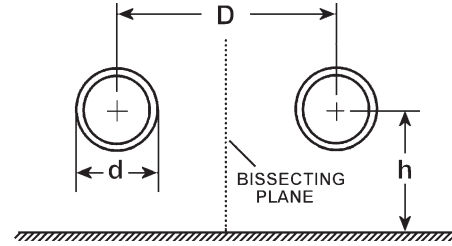


Fig. 12. Cross section of two circular coils near ground.

an inductance of the order of 1.01 mH. This agrees with the value of about 1.0 mH measured with an LC bridge multimeter.

The stray capacitance of the coaxial windings with respect to ground can be obtained from the known expression for the equivalent capacitance between two parallel circular conductors and the ground plane [17], [18], i.e.,

$$C \approx \frac{4\pi l \epsilon_0}{\ln \left\{ \frac{4h}{d} \sqrt{1 + \left(\frac{2h}{D}\right)^2} \right\}} \quad (\text{A2})$$

where $\epsilon_0 = 8.85 \times 10^{-12}$ F/m is the free-space permittivity, h is the distance between the coil axis and ground, and D is the separation between the active and passive coils as shown in Fig. 12. As the supporting structure of Fig. 3 is grounded, a pair of active and passive coils rests on a ground plane in each stage of the Blumlein structure. Taking $l \approx 100$ cm, $h = 21$ cm, $d = 40$ cm, and $D = 65$ cm in (A2) gives an estimated capacitance of a pair of coil shields near ground of the order of 124.4 pF. Since there is a bisecting plane between the coils, the capacitance between one coaxial winding and the ground plane is doubled, producing a capacitance of the order of 242.8 pF. The measurement of this capacitance with an LC bridge between one coil shield and the metallic plate gave a value of about 220 pF, which is in reasonable agreement with the calculation of the coil shield capacitance with respect to ground.

REFERENCES

- [1] F. Davanloo, C. B. Collins, and F. J. Agee, "High power repetitive stacked Blumlein pulsers commutated by a single switch element," *IEEE Trans. Plasma Sci.*, vol. 26, no. 5, pp. 1463–1475, Oct. 1998.
- [2] F. Davanloo, R. Dussart, K. J. Koivussari, C. B. Collins, and F. J. Agee, "Photoconductive switch enhancements and life time studies for use in stacked Blumlein pulsers," *IEEE Trans. Plasma Sci.*, vol. 28, pp. 1500–1506, Oct. 2000.
- [3] V. P. Singal and B. S. Narayan, "Development of a Blumlein based on helical line storage elements," *Rev. Sci. Instrum.*, vol. 72, no. 3, pp. 1862–1868, Mar. 2001.
- [4] I. C. Somerville, S. J. MacGregor, and O. Farish, "An efficient stacked-Blumlein HV pulse generator," *Meas. Sci. Technol.*, vol. 1, no. 9, pp. 865–868, Sep. 1990.
- [5] P. N. Graneau, J. O. Rossi, M. P. Brown, and P. W. Smith, "A high voltage transmission line transformer with very low droop," *Rev. Sci. Instrum.*, vol. 67, no. 7, pp. 2630–2635, Jul. 1996.
- [6] P. W. Smith and C. R. Wilson, "Transmission line transformers for high voltage pulse generation," in *Proc. 17th IEEE Power Modulator Symp. Conf.*, Seattle, WA, Jun. 1986, pp. 281–285.
- [7] C. R. Wilson, G. A. Erikson, and P. W. Smith, "Compact, repetitive, pulsed power generators based on transmission line transformers," in *Proc. 7th IEEE Pulsed Power Conf.*, Monterey, CA, Jun. 1989, pp. 108–112.
- [8] C. A. Pirrie, P. N. D. Maggs, and P. W. Smith, "A repetitive, thyatron switched, 200 kV, fast rise-time pulse generator, based on a stacked transmission line transformer," in *Proc. 8th Int. IEEE Pulsed Power Conf.*, San Diego, CA, Jun. 1991, pp. 310–314.

- [9] M. Rivaletto and P. Pignolet, "Characterization and realization of 120 kV, 200 ns transmission line pulse generator," *Eur. Phys. J., Appl. Phys.*, vol. 3, no. 2, pp. 159–167, Aug. 1998.
- [10] J. O. Rossi, I. H. Tan, and M. Ueda, "Plasma implantation using high-energy ions and short high voltage pulses," *Nucl. Instrum. Methods Phys. Res. B, Beam Interact. Mater. At.*, vol. 242, no. 1/2, pp. 328–331, Jan. 2006.
- [11] R. A. Fitch and V. T. S. Howell, "Novel principle of transient high-voltage generation," *Proc. Inst. Electr. Eng.*, vol. 111, no. 4, pp. 849–855, Apr. 1964.
- [12] J. O. Rossi, M. Ueda, and J. J. Barroso, "Design of a 150 kV, 300 A, 100 Hz, Blumlein coaxial pulser for long pulse operation," *IEEE Trans. Plasma Sci.*, vol. 30, no. 5, pp. 1622–1626, Oct. 2002.
- [13] J. S. Tyo, M. C. Skipper, and M. D. Abdalla, "Frequency and bandwidth Agile pulser for use in wideband applications," *IEEE Trans. Plasma Sci.*, vol. 32, no. 5, pp. 1925–1931, Oct. 2004.
- [14] *Pspice User's Guide*, Cadence Design Syst., Inc., Portland, OR, 2000.
- [15] J. Deng, R. H. Stark, and K. H. Schoenbach, "A nanosecond pulse generator for intracellular electro-manipulation," in *Proc. 24th Int. Power Modulator Symp. Conf.*, Norfolk, VA, Jun. 2000, pp. 47–50.
- [16] P. N. Graneau, J. O. Rossi, and P. W. Smith, "The operation and modeling of transmission line transformers," *Rev. Sci. Instrum.*, vol. 70, no. 7, pp. 3180–3185, Jul. 1999.
- [17] *Reference Data for Radio Engineers*, 5th ed. Indianapolis, IN: Sams, 1970, ch. 22.
- [18] A. D. Watt, *V. L. F. Radio Engineering*. Glasgow, U.K.: Pergamon Press, 1967, pp. 40–46.



José O. Rossi (M'05) was born in Amparo, SP, Brazil, in 1958. He received the B.Sc. degree in electrical engineering from the University of Campinas, Campinas, SP, Brazil, in 1982, the M.Sc. degree in electronics from the Technological Institute of Aeronautics, São José dos Campos, SP, Brazil, in 1992, and the Ph.D. degree in engineering science from Oxford University, Oxford, U.K., in 1998.

He has been with the National Institute for Space Research (INPE), São José dos Campos, since 1983, working on pulsed-power generators for microwave devices and plasma immersion ion implantation experiments. From 1994 to 1998, he was engaged in Ph.D. research on pulsed-power systems and transmission-line pulse transformers at the Department of Engineering Science, Oxford University. His current research interests include the development of new pulsed power systems applied in plasma technology devices and plasma ion implantation.

Dr. Rossi is a member of the Brazilian Power Electronics and Physical Societies and a Consultant on research projects for the Assisting Research Foundation of the Parana State and the State of Sao Paulo Research Foundation (FAPESP), Brazil.



Joaquim J. Barroso received the B.Sc. degree in electrical engineering and the M.Sc. degree in plasma physics from the Technological Institute of Aeronautics, São José dos Campos, SP, Brazil, in 1976 and 1980, respectively, and the Ph.D. degree in plasma physics from the National Institute for Space Research (INPE), São José dos Campos, in 1988.

He has been with INPE since 1982 and has been involved in the design and construction of a high-power 32-GHz gyrotron. During 1989–1990, he was a Visiting Scientist with the Plasma Fusion Center, Massachusetts Institute of Technology, Cambridge. His current interests include high-power microwave generators and plasma technology.

Mário Ueda was born in Sao Paulo, Brazil, on August 16, 1951. He received the B.Sc. degree in physics from the University of Sao Paulo, in 1974, the M.Sc. degree from Nagoya University, Nagoya, Japan, in 1978, and the Ph.D. degree from Cornell University, Ithaca, NY, in 1986.

During 1990–1991, he was a Visiting Scientist with the National Institute for Fusion Science, Japan. Since 1978, he has been with the National Institute for Space Research (INPE), São José dos Campos, SP, Brazil. His current research interests include plasma immersion ion implantation, diagnostics of high- and low-temperature plasmas using neutral lithium beam technique, high-power pulsed systems, and material processing by plasma and ion implantation.